INTERNATIONAL ATOMIC ENERGY AGENCY
UNITED NATIONS EDUCATIONAL, SCIENTIFIC AND CULTURAL ORGANIZATION
INTERNATIONAL CENTRE FOR THEORETICAL PHYSICS
I.C.T.P., P.O. BOX 586, 34100 TRIESTE, ITALY, CABLE: CENTRATOM TRIESTE

SMR/388 - 45

SPRING COLLEGE IN MATERIALS SCIENCE
ON
'CERAMICS AND COMPOSITE MATERIALS'
(17 April - 26 May 1989)

POSITRON STUDIES ON DEFECTS IN MATERIALS

CHI WEI LUNG
Institute of Metal Research
Academia Sinica
Wenhua Road
Shenyang
People's Republic of China

POSITRON STUDIES on DEFECTS in MATERIALS

I. Introduction to PA

Special advantages:

Sensitive to the presence of defects.

$\sim 10^{-7}$ vacancy concentration, $\sim 10^{3}$ voids ($\sim$ 45Å)

For studies of nondilute alloys

$> 1\% \rightarrow 100\%$

For studies under wide range temperatures

Wide range of fields

metals, semiconductors, ionic solids, polymers....

mechanical engineering, materials science,

solid state physics, theoretical physics...

Not very expensive

~ US $ 20,000 - 40,000.

Disadvantages:

Use of radioactive materials.

Complicated data analysis for the lifetime technique.

Unconventional instrumentation for many metallurgy and chemistry laboratories.

Reduced sensitivity for complicated materials (trapping saturation).

Need for a standard in order to calibrate in terms of defect concentration.

Examples of successful work:

Most reliable values of single-vacancy formation enthalpy (also in refractory metals)

Detection of microvoids and void precursors produced by low-dose neutron irradiation (below TEM resolution)

Firm experimental evidence of a vacancy migration mechanism for III stage annealing in plastically deformed iron.

References

1. P. Hautojärvi, Positrons in Solids, Springer, Berlin, 1979.

2. W. Brandt and A. Dupasquier, Positron Solid State Physics, Proc. Inter. Sch. Phys. "Enrico Fermi", North-Holland Publ. Co. (1983).

3. P.C. Jain, R.M. Singru and K.P. Gopinathan, Positron Annihilation, Proc. ICPA-7. World Scientific, (1985).

4. C.W. Lung and N.H. March, Cryst. Latt. Def. and Amorphous Materials. 13 (1986) 31.

5. Proc. ICPA-8. Gent, (in press). 1988.

I. 1. Thermorlization

e^+ Source: ^{22}Na, ^{64}Cu, ^{58}Co, ^{68}Ge — γ-ray (^{22}Na)
(0.54 Mev) (0.65) (0.48) (1.4) (1.28 Mev)

time: $\sim 10^{-12}$ sec.

distance: $10 - 1000$ μm.

energy: $kT(\sim 30^\circ c) \sim 0.025$ ev.

2. Annihilation. ($\frac{v}{c} << \alpha = \frac{1}{137}$)

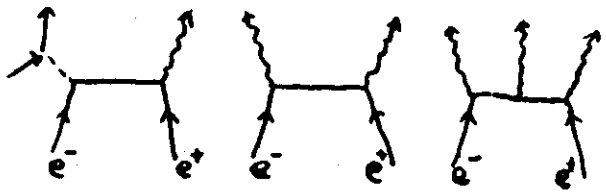

$\sigma_{(2)}/\sigma_{(2)} \approx \alpha$. $\quad \sigma_{(3)}/\sigma_{(2)} \approx \alpha^2$

$\sigma_{(2)} = \frac{\pi r_0^2 c}{v}$

$\Gamma_{(2)} = \sigma_{(2)} v n_e = \pi r_0^2 c n_e$

$2 m_0 c^2 = 2 \times 0.511 \times 10^6$ ev $\quad \gamma$

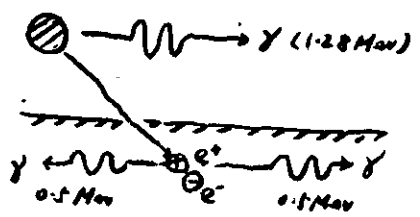

II, Lifetime $\tau = \Gamma^{-1}$

	Solid	Liquid	Gas
τ (sec)	$\sim 10^{-10}$	$\sim 10^{-9}$	$\sim 10^{-7}$

$\tau_p < \tau_d$

III. Angular correlation

e^-, e^+ static: $\vec{P}_1 + \vec{P}_2 = 0$; $\vec{c}_1 = -\vec{c}_2$; 180°

e^- motion: $\vec{P}_1 + \vec{P}_2 \neq 0$ $\quad \vec{c}_1 \neq -\vec{c}_2$; θ_{12}

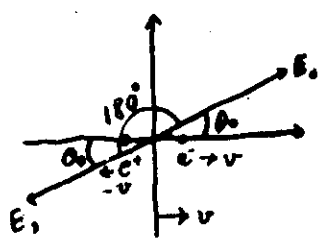

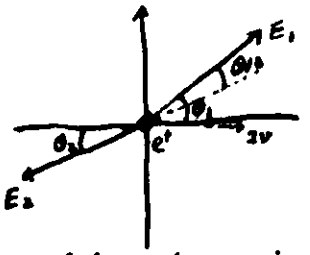

(a) axis system of center of mass (b) Laboratory axis system.

$\sum P_i = m(v_1 + v_2) = m(-v + v) = 0$

$\theta_{12} \approx \tan(\theta_1 - \theta_2) \approx \frac{\frac{2v}{c} \sin\theta_0}{1 - v^2/c^2} = \frac{2v}{c} \sin\theta_0 = \frac{P_T}{m_0 c}$

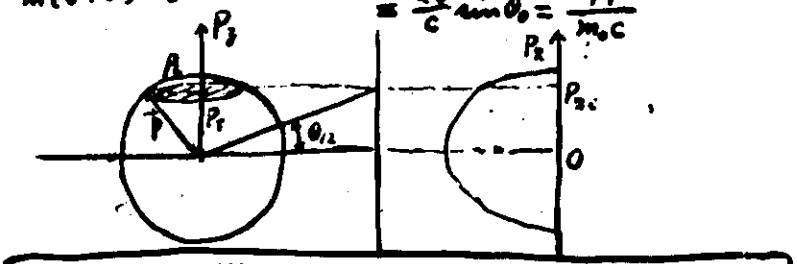

$$N(\theta_2) = c \int_{-\infty}^{+\infty} \int_{-\infty}^{\infty} dp_x\, dp_y\, \Gamma(p_x, p_y, \theta_2, m_0 c) = N(p_x)$$

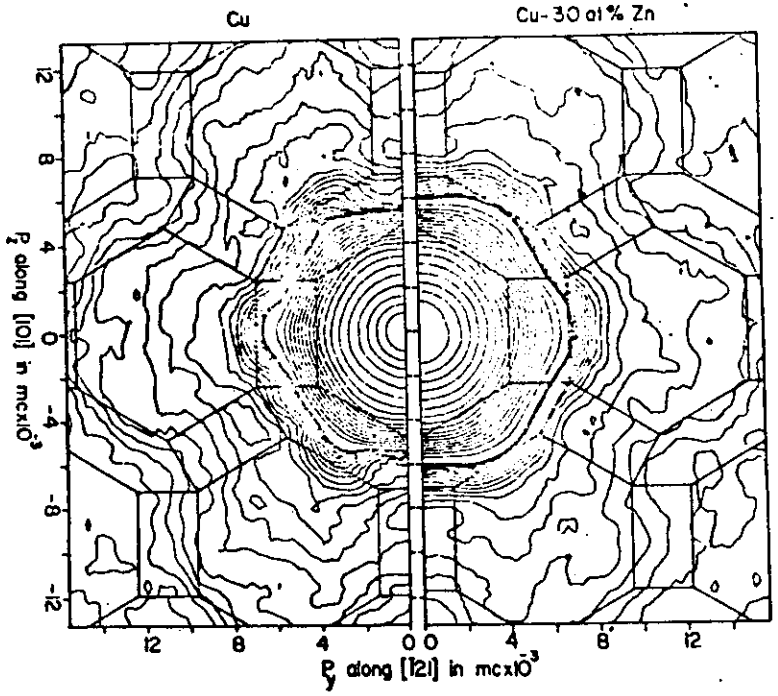

Fig. 13 The contour map of the $N(p_yp_z) - R(p_yp_z)$ surface from Cu vs Cu-30 at.% Zn, oriented with p_x along the [111] direction. $R(p_yp_z)$ is a smooth rotationally symmetric surface as discussed in the text, used to exhibit the anisotropies at high momenta.

We have applied our 2D technique to the study of α-brass. Full 2D ACAR surfaces have been measured for Cu-11.6 at.% Zn [59] and Cu-30 at.% Zn, and have been compared to pure Cu [60]; we find that the momentum density is quite similar between α-brass and pure copper, except for the clear growth of the FS with alloying. We demonstrate this similarity in Fig. 13, where the contour maps of $N(p_yp_z) - R(p_yp_z)$ have been plotted for Cu and Cu-30 at.% Zn for p_x along the [111] direction (corresponding to the orientation in Fig. 6). The isotropic R for Cu was the same as used in Fig. 9; the same shaped R but with a 12% reduced amplitude was used for Cu-30 at.% Zn. We note the clear growth of the FS features in the first zone. The anisotropy in higher zones is quite similar between Cu and the Cu-30 at.% Zn sample. In order to analyze qualitatively these 2D ACAR surfaces we construct from the raw $N(p_yp_z)$ a set of radial distributions $N(p,\theta)$ in the (p_yp_z) plane by linear interpolation, and differentiate these distributions to obtain the breaks due to the FS. After applying resolution corrections to this analysis

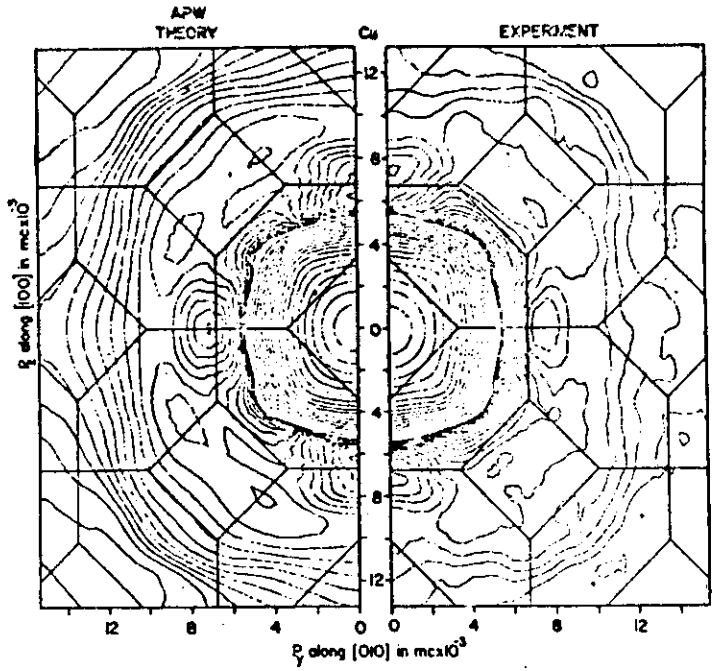

Fig. 9 Contour maps of experimental vs theoretical $N(p_yp_z) - R(p_yp_z)$ for Cu with p_x along the [001] direction. $R(p_yp_z)$ is a smooth rotationally symmetric surface as discussed in the text, and is used to exhibit the anisotropies at high momenta. The steps of the contour lines are changed at around p - 5.5 mrad as discussed in the text.

ACAR — Angular correlation annihilation radiation

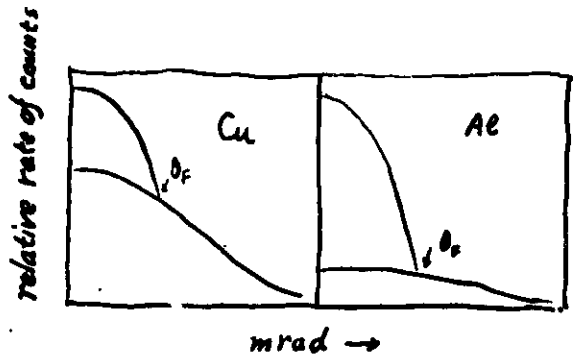

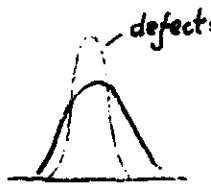

IV. Doppler broadening

$$E_{1,2} \approx \frac{1}{2} E_\gamma' \left(1 \pm \frac{v}{c}\cos\theta_0\right)$$

$$\approx m_0 c \pm \frac{c P_L}{2} = E_0 \pm \delta E$$

$$P_L = 2 m_0 v \cos\theta$$

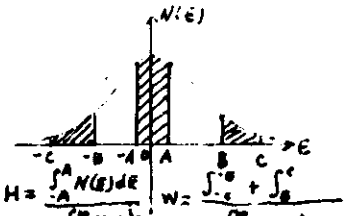

V. Interaction between e^+ and vacancy

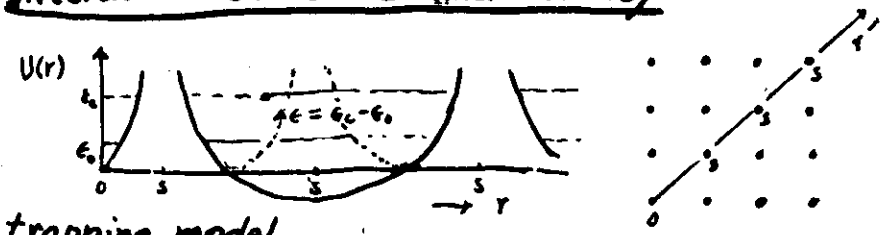

VI. trapping model

$$\frac{dn_f(t)}{dt} = -\left(\frac{1}{\tau_f} + \sum_{j=1}^{m} \sigma_j(t) C_j\right) n_f(t) + \sum_{j=1}^{m} \nu_j n_j(t)$$

$$\frac{dn_j(t)}{dt} = -\frac{n_j(t)}{\tau_j} + \sigma_j(t) C_j n_f(t) - \nu_j n_j(t)$$

$(j = 1, 2, \cdots, m)$

Assuming: $\nu_j = 0$ (no detrapping) A. Seeger (J. Phys. F. 3 (1973) 248)

$\sigma_j(t) = \sigma_j$

The solution is

$$n_f(t) = n_f(0) \exp(-t/\tau_0)$$

$$\left(\frac{1}{\tau_0} = \frac{1}{\tau_f} + \sum_{j=1}^{m} \sigma_j C_j\right)$$

$$n_j(t) = \tau_0 \tau_j \frac{\sigma_j C_j}{\tau_0 - \tau_j} n_f(0) \exp(-t/\tau_0) +$$

$$\left[n_j(0) - \tau_0 \tau_j \frac{\sigma_j C_j}{\tau_0 - \tau_j} n_f(0)\right] \exp(-t/\tau_j)$$

$j = 1, 2, \cdots m.$

For spherical attractive potential wells, one obtains

$$\sigma_j(t) = \frac{4\pi r_j D}{\Omega}\left[1 + r_j (\pi D t)^{-\frac{1}{2}}\right]$$ Waite's theory

or $$\sigma_j(t) \approx \frac{4\pi r_j D}{\Omega}$$

where Ω is the atomic volume, and D the diffusion coefficient.

$$k = \left\{\begin{matrix}\sigma \\ \mu\end{matrix}\right\} C_t$$

k: trapping rate; σ, μ: specific; C_t: concentration of traps of type j

$$\bar{\tau} = \frac{\int_0^\infty [n_f(t) + \sum_{j=1}^{m} n_j(t)]\,dt}{n_f(0) + \sum_{j=1}^{m} n_j(0)}$$

$$\bar{\tau} = \tau_f \cdot \frac{1 + \sigma \tau_f C_{iv}}{1 + \sigma \tau_f C_{iv}} \quad \text{(for monovacancy)}$$

or: $\dfrac{\bar{\tau} - \tau_f}{\tau_e - \tau_f} = \dfrac{\sigma C_{iv}}{1 + C_{iv}\sigma}$; $\boxed{\dfrac{\bar{\tau} - \tau_f}{\tau_e - \bar{\tau}} = \tau_f \sigma_i C_{iv}}$.

$$\sigma = \frac{4\pi D r_{iv}}{\Omega}$$

$$\bar{\tau} = \tau_f \cdot \frac{1 + (4\pi r_{iv} C_{iv} \tau_{iv} D/\Omega)}{1 + (4\pi r_{iv} C_{iv} \tau_f D/\Omega)}$$

$$C_{iv} = \exp(S_{iv}^f/k) \exp(-H_{iv}^f/kT)$$

$$\boxed{H_{iv}^f = kT\left[\frac{S_{iv}^f}{k} + \ln\left(\frac{4\pi D}{\Omega} r_{iv} \tau_f\right) + \ln\left(\frac{\tau_{iv} - \bar{\tau}}{\bar{\tau} - \tau_f}\right)\right]}$$

(vacancy formation energy)

VII.

$$\Gamma_0 = \pi r_0^2 c\, n_e$$

$$\Gamma_0(p) = (\pi r_0^2 c)\frac{1}{(2\pi)^3}\sum_i \left| \int d\underline{r}\, \exp(-i\underline{p}\cdot\underline{r})\psi_i(\underline{r})\psi_i^*(\underline{r}) \right|^2$$

$\psi(\vec{r})$: electron wave function

$\psi_+(\vec{r})$: positron wave function

$r_0 = e^2/mc^2$: the classical electron radius.

VIII. e^+ and defects

$H\psi_+(\vec{r}) = E_0 \psi_+(\vec{r})$

pseudopotential and pseudo wave function

1. $\psi_{\underline{k}}(\underline{r}) = U(\underline{r} - \underline{R})\,\varphi_{\underline{k}}(\underline{r})$ (perfect crystal)

$$\left[-\frac{\hbar^2}{2m}\frac{\partial^2}{\partial r^2} + V_a(r)\right] U(r) = E_{wi}\, U(r)$$

$$\left.\frac{\partial U}{\partial r}\right|_{r=R_0} = 0 \qquad R_0 : \text{muffin-tin radius}$$

$$\left[-\frac{\hbar^2}{2m}\nabla^2 + w(\underline{r})\right]\varphi_{\underline{k}}(\underline{r}) = E_0(\underline{k})\,\varphi_{\underline{k}}(\underline{r})$$

where,

$$w(\underline{r}) = \begin{cases} E_{wi} + V(\underline{r}) \oplus V_a(\underline{r} - \underline{R}) - \dfrac{\hbar^2}{m}\dfrac{\nabla U(r)}{U(r)} \cdot \nabla & (\text{in}) \quad (w < v) \\ V(\underline{r}) & (\text{between}) \end{cases}$$

2. defect crystal

$$V(\underline{r}) = \sum_i V_{vaj}(\underline{r} - \underline{R}_j) + \Delta V(\underline{r}) + V_{corr}(\underline{r})$$

$$V_{vaj}(\underline{r}) = \begin{cases} V_{aj}(\underline{r}), & (\text{in}) \\ 0, & (\text{outside}) \end{cases}$$

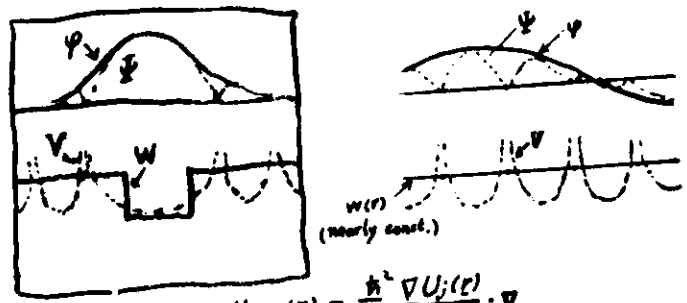

$$w(\underline{r}) = \Delta V(\underline{r}) + E_{wi} + V_{corr}(r) - \frac{\hbar^2}{m}\frac{\nabla U_i(r)}{U_i(r)} \cdot \nabla$$

IX. Annihilation characteristic

1-D angular correlation curve

$$I(p_z) = \int dp_x \int dp_y \, \Gamma_0(p)$$

isotropic : e^+-e^- overlaping integral

$$I(p_z) = 2\pi \int_{p_z}^{\infty} dp \cdot p \, \Gamma_0(p)$$

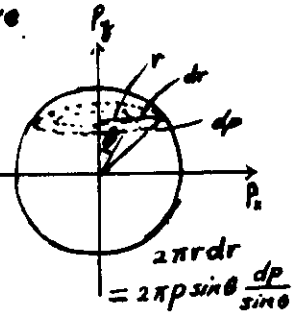

$2\pi r dr = 2\pi p \sin\theta \frac{dp}{\sin\theta} = 2\pi p \, dp$

homogeneous electron gas: $\Gamma_0(p) = \frac{\pi r_0^2 c}{(2\pi)^3}$

$$I(p_z) = \frac{r_0^2 c}{4\pi}(p_F^2 - p_z^2)\,\theta(p_F - |p_z|)$$

($|p_z| < p_F$ 일 때, $\theta(p_z) = 1$; $|p_z| > p_F$ 일 때, $\theta(p_z) = 0$)

inhomogeneous electron system:

$$I(p_z) = \frac{\pi r_0^2 c}{4\pi} \int d\underline{r} \, |\psi(\underline{r})|^2 \lambda[n(\underline{r})]$$

where, $\lambda[n(\underline{r})] \underset{\lambda}{\overset{n(\underline{r})}{=}} [p_F(\underline{r})^2 - p_z^2]\,\theta(p_F(\underline{r})^2 - |p_z|^2)$

Vacancy studies with PA (Experiment)

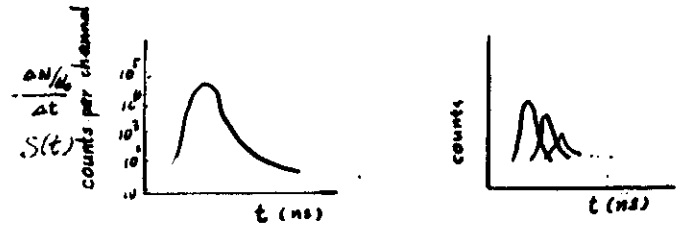

The resulting experimental time spectrum $S(t)$ can be written as the sum of n components

$$S(t) = \sum_{i=1}^{n} I_i \Gamma_i e^{-\Gamma_i t}$$

For simplicity, we discuss the two state trapping model.

$$S(t) = I_1 \Gamma_1 e^{-\Gamma_1 t} + I_2 \Gamma_2 e^{-\Gamma_2 t}$$

$$\Gamma_1 = \lambda_f + k = \tau_1^{-1} \qquad I_1 = \frac{\lambda_f - \lambda_t}{\Gamma_1 - \lambda_t}$$

$$\Gamma_2 = \lambda_t = \tau_2^{-1} \qquad I_2 = \frac{k}{\Gamma_1 - \lambda_t}$$

($\lambda_f = \tau_f^{-1}$, $\lambda_t = \tau_t^{-1}$, $k = \sigma C_t$)

$$\sigma C_t = I_2 \left(\frac{1}{\tau_1} - \frac{1}{\tau_f} \right)$$

$$C_t = \exp(S_N^F / k_B) \exp(-H_N^F / k_B T)$$

$$C_t \equiv C_{iv} = \exp(S^F_{iv}/k_B)\exp(-H^F_{iv}/k_BT)$$

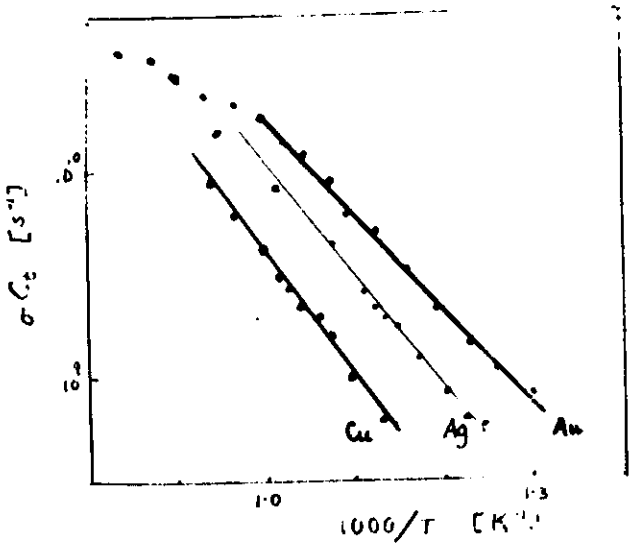

Fig. Arrhenius plots of the trapping rates σC_t with T^{-1}

Proc. ICPA-7 (1981) 456
Stuck and Schaefer

Table: Vacancy formation enthalpies H^F_{iv} by PA

Metal	H^F_{iv} (ev)	Metal	H^F_{iv} (ev)
Mg	0·85 ± 0·10	Ta	2·8 ± 0·6
Al	0·68 ± 0·04	Cr	2·0 ± 0·2
In	0·55 ± 0·03	Mo	3·0 ± 0·2
Cu	1·29 ± 0·07	W	4·0 ± 0·3
Ag	1·12 ± 0·07	α-Fe	1·6 ± 0·15
Au	0·89 ± 0·04	Co	1·34 ± 0·07
Zn	0·52 ± 0·07	Ni	1·78 ± 0·10
Cd	0·52 ± 0·02	Pd	1·85 ± 0·25
Pb	0·57 ± 0·06	Pt	1·32 ± 0·04
V	2·1 ± 0·20	Sn	0·50 ± 0·01
Nb	2·65 ± 0·40	U	≃ 1·0

Proc. ICPA-7 (1981) 448
Schaefer

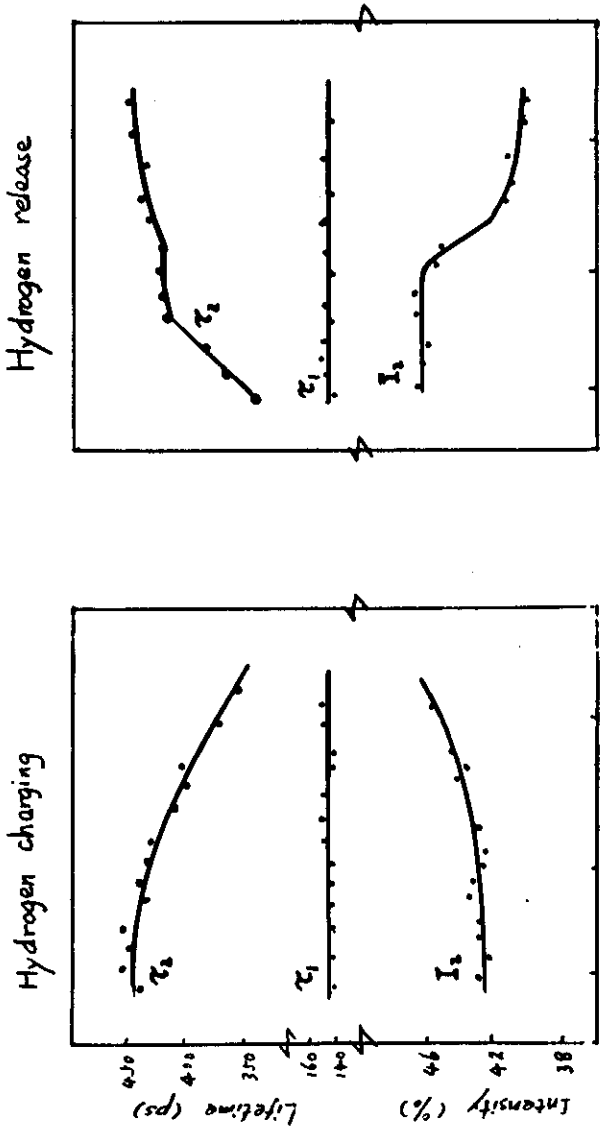

Fig. Positron lifetime parameters in Mo containing voids (T_{prep} = 450°C) during electrolytical H injection (uncal. scale) and thermal H release.

Proc. ICPA-7 (1981) 497
B. Nielsen et al.

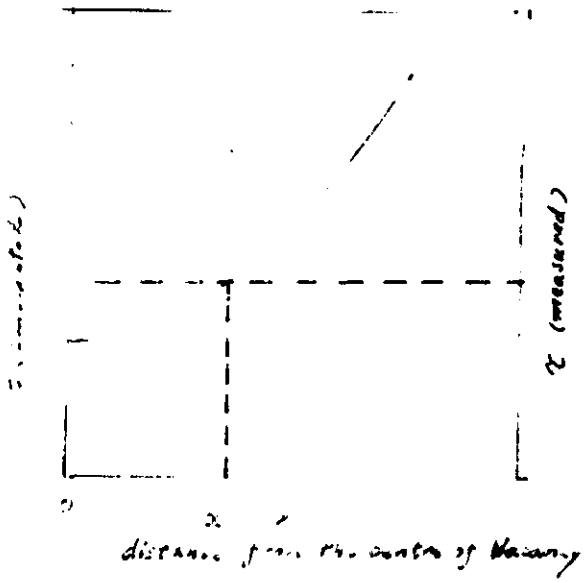

The position of the atom of the impurity atom-decorated vacancy can be determined by combination of theoretical calculation and PA lifetime measurements.

DISLOCATION TRAPS

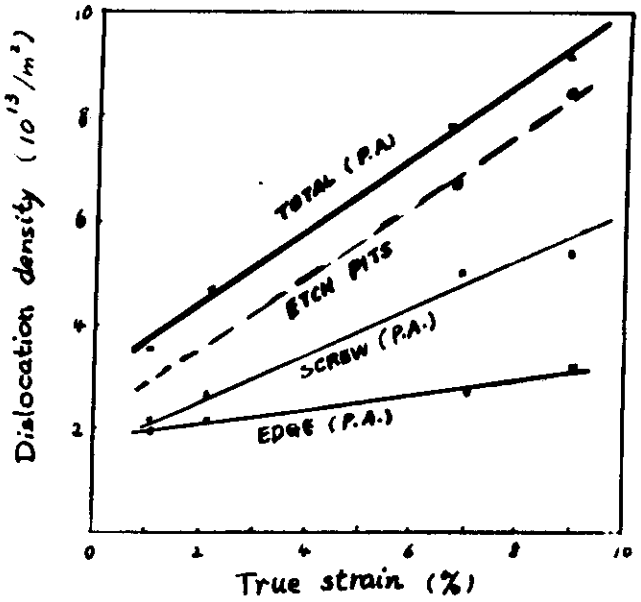

Fig. Dislocation densities measured by PA and etch pits in iron single crystals in tension at 200 K.

$\tau_s = 142 \pm 5$ ps.

$\tau_e = 165 \pm 3$ ps.

$\varepsilon < 10\%$ $\qquad \sigma = K_t/C_t \simeq (1\text{-}10) \times 10^{-5}$ m/

$\tau_j = 114$ psec

jog separation : 2000 b (by TEM)

no. of jog traps / total traps $\lesssim 10^{-3}$

The unresolved (small) jogs can not be ruled out as being the sites for PA.

ICPA-7 (1984) 487
Y.H. Park et al.

P-N dislocation core model and positron annihilation effects

位错中心 P-N 模型和正电子湮没效应

$$u_x = -\frac{b}{2\pi}\tan^{-1}\left(\frac{x}{\zeta}\right)$$

ζ, semi width of the disl. simple 2-D model

ζ 是位错半宽度. 二维的简化模型.

$$u_y = -(b/2\pi)\tan^{-1}\left(\frac{y}{\zeta}\right)$$

$$u_\theta = 0$$

位错中心的体积膨胀 volume expansion in the dislocation core

$$f(r) = \operatorname{div} \underline{u}$$

$$= -(b/2\pi r)\tan^{-1}\left(\frac{r}{\zeta}\right) - \frac{b}{2\pi\zeta}\frac{1}{1+\left(\frac{r}{\zeta}\right)^2}$$

$$\rho_i(r) = \rho_0[1+f(r)]$$ (位错心离子密度) ion density in the disl. core

$$= \rho_0\left[1 - \frac{b}{2\pi r}\tan^{-1}\frac{r}{\zeta} - \frac{b}{2\pi\zeta}\frac{1}{1+\left(\frac{r}{\zeta}\right)^2}\right]$$

$$\Delta\tau = \tau_d - \tau_f = 15\ ps\ ; \quad E_b \approx 1.1\ ev$$

compare with binding energy due to vacancy

$$E_b^v = 2.2\ ev$$

Shen J.Q., LUNG C.W., Wang K.L. Proc. ICPA-7 (1985) phys. stat. sol. (b) 134, (1986).

compare with Martin and Puska: results of disl. (1972)

$$E_b^d \approx 0.1\ ev.$$

compare with Arponen et al. (1973)

$$E_b^d = 2.79\ ev.$$

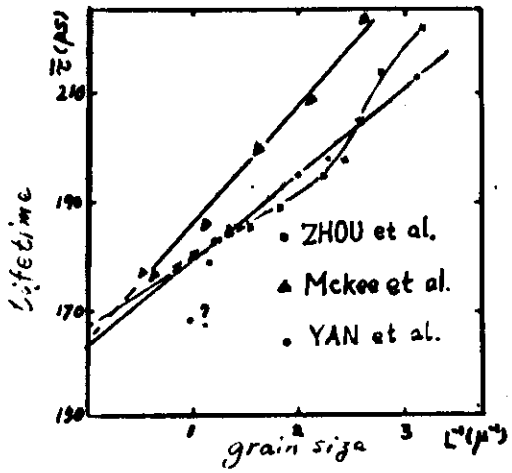

Zn - 22 wt.% Al

Heat treatments and measured results

编号	热处理方法 Temp.	Time	quenching	grain size	lifetime
	加热温度	保温时间	淬火方式	ℓ (μm)	τ (ps)
6	360°C	0.5hr.	冰盐水淬	0.82	213
2	350°C 250°C	0.5hr.	冰盐水淬 空冷	0.39	205
1	350°C 250°C	0.5hr.	冰盐水淬	0.44	198
15	250°C	0.5hr.	炉冷	0.80	195
3	350°C 250°C	0.5hr.	冰盐水淬 水淬	0.76	185
14	250°C	0.5hr.	空冷	0.86	179
12	250°C	0.5hr.	油淬	1.02	168
16	试样初态			0.80	183

(周先意、王淑英、蒋惠林、姜 依、龙期威), 1984.
ZHOU, WANG, JIANG, JIANG, LUNG
YAN D. XIONG L.Y. & LUNG C.W. 1988.

裂缝顶端范性区的正电子湮灭

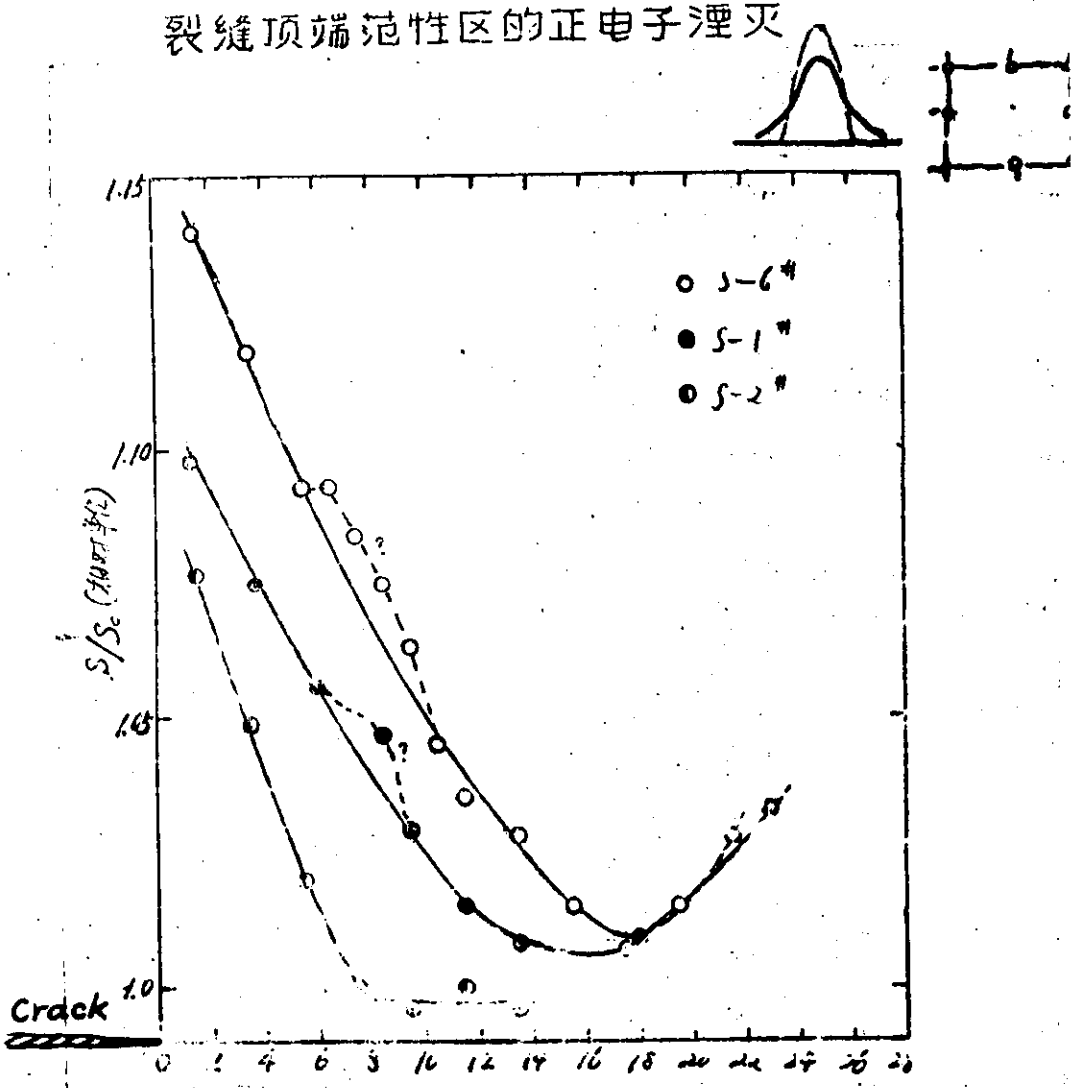

Positron annihilation in the plastic zone at a crack tip

in «Positron Annihilation», (1982) 469, North-Holland Publ. (Jiang, Xiong, Lung et al.)

1981.6.

1, Dislocations and vacancies were mixed.

2. can not see DF2

3. can measure the plastic zone size*

* Xiao Jimei et al. Script. Met. 1:12

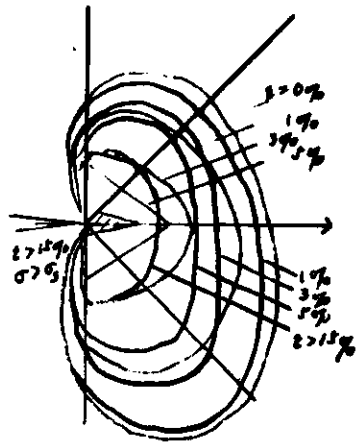

Fig. The H effects on the plastic zone of cracked 40MnNb steel measured by PA.

Tien Z. et al. Scripta Met., 16 (1982), 1383

Fatique:

L. Diaz, R. Pareja et al. Proc. ICPA-7 (1985) 579.
L. Diaz, R. Pareja et al. Phil. Mag. A51, 6 (1985) L61.
S. Y. Wang et al. Proc. ICPA-7 (1985) 467.

Wang et al: (Ni polycrystalline)

1. multi-exponential fitting method. (3)
2. τ_1^0 : e^+ free lifetime.
3. τ_{2A}, τ_{2B} 209-255 ⇒ 340 ps — $\log N$ (N: 10→10^6) vacancy clusters
4. τ_{1A}, τ_{1B} saturation value ~ 168 ps dislocation loop / vacancy
5. $\tau_3^0 = \tau_{3A}' = \tau_{3B}$ due to specimen surface.

Diaz et al.

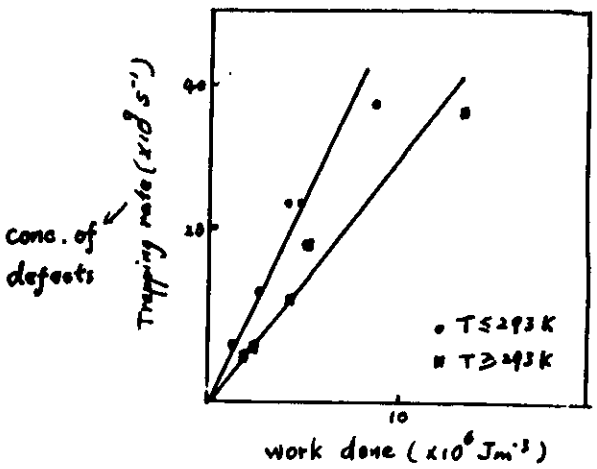

Nanocrystalline iron

(H. E. Schaefer and R. Würschum, 1986)
(Preprint)

Small crystallite sizes: 5 - 10 nm (0.005 - 0.01 μm)

1. volume fraction of interfacial structure
   20 - 50 % (3 - 10 nm)

2. τ_1 is similar to the lifetime τ_{1V} = 175 ps observed as at monovacancies in bulk iron.

3. τ_1 persist up to temperature T = 320°C (not recover below this temperature)

4. τ_2 is attributed to positron trapping at microvoids at the intersection of several crystalline interfaces. (τ_2 also persists up to temperature T = 320°C)

positronium in molecular materials (Wallace, 1960).

$$V_e > E > V_i - 6.8\ eV \quad \text{(Ore Gap)}$$

V_i: Ionization potential of a molecule of the medium
V_e: the lowest excitation potential.
6.8 eV: the binding energy of the ps atom.

Ps in ionic crystals.

$(e^+ e^-)$

$$V_1 > E > (V_i + Q_p) - (B.E. + Q_{ps})$$

V_1: energy required to promote an electron to the unoccupied state of lowest energy.
Q_p: energy required to remove a thermalized positron from the system.
Q_{ps}: that for the ps atom.

Let $Q_e = V_i - V_1$ (the electron affinity of the crystal.

The criterion for the existence of the Ore gap:

$$Q_e + Q_p < Q_{ps} + B.E.$$

The complexity of positron state in ionic materials

1. Thermalization of e^+ may not be completed in some materials.
2. Formation of ps atom
   - moderate more slowly (~300 ps).
   - ratio of 3γ to 2γ annihilation for ps will be larger
3. Lifetime spectra are more complex than in metals. the cause of the complexity is not clear. (3 2 states) pure bulk effect? lattice defect trapping?
4. e^+ with a preference for negative ion cells and for interstitial regions.

	$R = S^+/S^-$
LiF	0.08
LiCl	0.05
NaCl	0.10
KCl	0.13
KI	0.13

(S^+: overlap on cation
S^-: " " anion)

5. Positronium-like state
   e^+ - negative ion bound state.

e^+ trapping at vacancies in Si

- lifetime increases linearly
- does not seem to show any saturation at 500 ps. (comparing to metals)

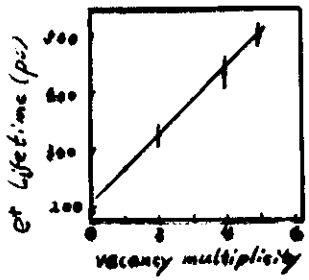

- $\tau_{1v}/\tau_b \sim 1.23$
  (less than in metals, indicating weaker positron binding and localization at monovacancy.)
- The e^+ trapping mechanism is an open problem! trapping may depend on temperature and the charge state of a defect.

e^+ trapping at F-centres in ionic crystals

Substance	F-centre density (10^{17} cm^{-3})	τ (ns)	I (%)	κ
NaCl	0.5	1.09 ± 0.02	4 ± 1	< 1
KCl	1	0.99 ± 0.02	21 ± 1.5	0.29 ± 0.04
KBr	4.5	1.06 ± 0.02	28.8 ± 0.3	0.48 ± 0.05
KI	2	1.46 ± 0.04	6.5 ± 0.3	0.09 ± 0.01

$$e^+ + \text{F-Centre} \rightarrow {}^4A^+$$

Slow positron beam:

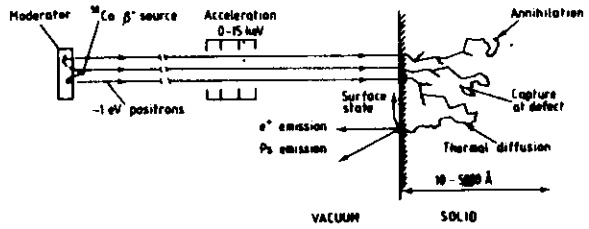

Fig. 9. Schematic view of a slow positron beam and positron surface processes.

The thermalized positrons diffuse in the lattice

1. Annihilate as free particles.
2. Be trapped at a defect.
3. Reach back to the entrance surface.

The $3\gamma/2\gamma$ ratio gives an experimental measure to the fraction of Ps emission, which is proportional to the number of positrons diffused back to the surface.

Comparing the number of e^+ reaching back to the surface in the sample with and without defects one can deduce the fractions of trapped e^+ at various beam energies.

P. Hautojärvi, Mat. Res. Symp. Proc.

Ar^+ sputtered Mo(111)

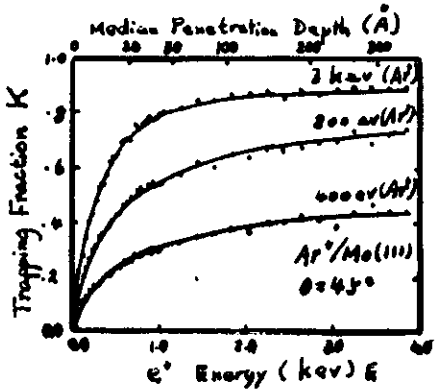

E: Positron beam energy

K(E): Fraction of trapped positrons

1. The mean positron implantation depth in Mo increases with incident energy.

2. At moderate energies, (E > 1kev), K also increases rapidly. (deeper depth)

3. At higher energies, K(E) becomes a constant. (defect distribution of finite depth)

4. The asymptotic value of K ~ total number of defects integrated over the depth direction.

e^+ in $YBa_2Cu_3O_{7-x}$

Zhang, Mao, Zhu, Lung, Proc. ICPA-8 (1988), Gent.

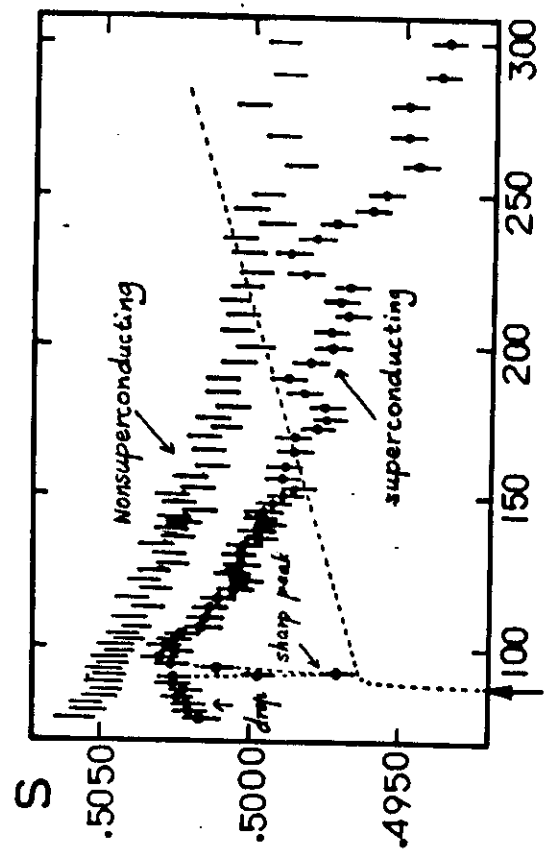

1. different temperature dependence near and below Tc (e^+ delocalized between Cu-O
2. A sharp peak near Tc (also a internal friction peak) during structural transition
3. The complexity of the structure and questions of ionicity and covalency in the bonds in complex samples (pure and simple structure samples needed).

Fig. 21

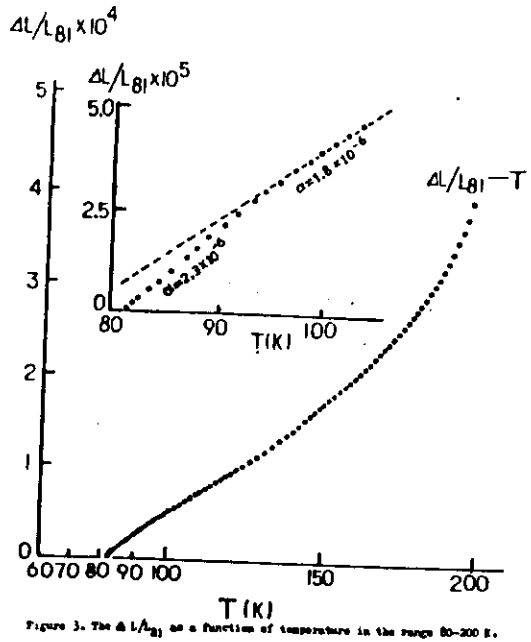

Figure 3. The $\Delta L/L_{81}$ as a function of temperature in the range 80–200 K.

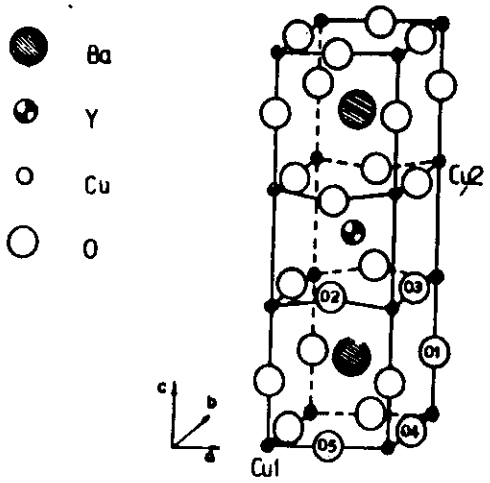

Figure 2. The crystal structure of $YBa_2Cu_3O_{7-x}$.

ZHANG, ZHU, LUNG et al., Proc. ICPA-8, (1988) Gent.

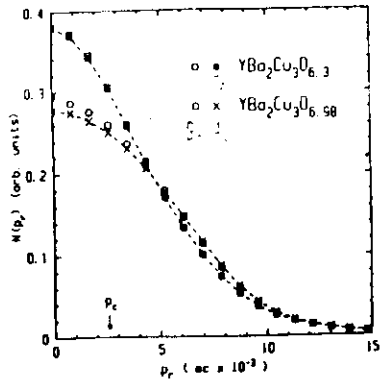

FIG. 1. Room-temperature radial distributions $N(p_z)$ of the 2D ACAR data for four $YBa_2Cu_3O_{7-x}$ samples described in text: crosses, A_6; circles, B_6; filled squares, C_{∞}; and open squares, D_{∞}. $p_z = 2.6 \times 10^{-3}$ marks the cutoff momentum described in text.

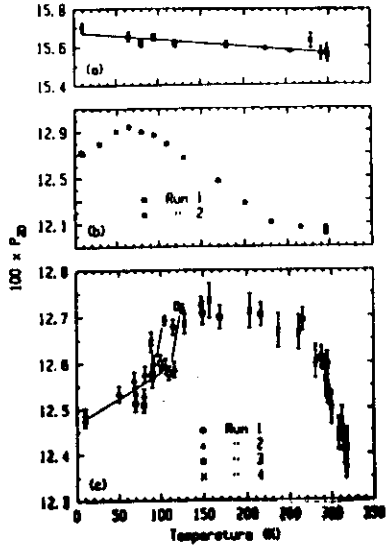

FIG. 2. Temperature dependence of the 2D shape parameter P_{SD} defined in text. (a) Nonsuperconducting sample D_{∞} and the linear fit described in text. (b) Superconducting sample A_6 for two warming cycles. (c) Superconducting sample B_6 for four warming cycles; lines are drawn to guide the eye.

von Stetten, Berko, Li, Lee, et al.
High Sensitivity of Positrons to Oxygen Vacancies and to Cu-O Chain Disorder in $YBa_2Cu_3O_{7-x}$
PRL, (1988), 2198.

ICPA-8 . (19**), Gent.

POSTERS: SEMICONDUCTORS

G01: "Positron studies of vacancies in semiconductors"
R.Würschum, W.Bauer, K.Maier, J.Major, A.Seeger, H.Stoll,
H.D.Carstanjen, W.Decker, J.Diehl, H.E.Schaefer

G02: "Phonon-cascade model of positron trapping in structural defects in semiconductors"
E.Boronski, R.M.Nieminen

G03: "LCAO calculations of momentum densities in some semiconductors"
T.Chiba, T.Akahane

G04: "Temperature dependent positron diffusion in semiconductors"
M.Singh, S.Y.Tang

G05: "Vacancy-type damage profiles in ion-implanted silicon studied by slow positron beam"
P.Hautojärvi, P.Huttunen, J.Mäkinen, A.Vehanen

G06: "Positron annihilation study of defects in electron irradiated silicon"
Motoko-Kwete, D.Segers, M.Dorikens, L.Dorikens-Vanpraet, P.Clauws, I.Lemahieu

G07: "Positron lifetime in electron irradiated silicon"
P.Moser, J.Mäkinen, C.Corbel, P.Hautojärvi, F.Pierre

G08: "Ion-implantation-induced damage in Si studied by monoenergetic positrons"
A.Uedono, S.Tanigawa, J.Sugiura, M.Ogasawara

G09: "Positron energy bands and wave functions in a Si crystal"
C.Pennetta, A.Baldereschi

G10: "Measurement of positron mobility in silicon by a lifetime method"
R.I.Simpson, M.G.Stewart, C.D.Beling, M.Charlton

G11: "Non-destructive testing of silicon single crystals by positron annihilation"
M.Doyama, Y.Suzuki, S.Ishibashi, T.Abe, M.Harada

G12: "Defect profiling in MBE-grown Si/Si(100) epilayers"
E.Tandberg, P.J.Schultz, T.E.Jackman, M.W.Denhoff

G13: "The accumulation and inversion states of SiO2/Si interface of MOS
structure investigated by a variable-energy positron beam"
A.Uedono, S.Tanigawa, Y.Ohji

G14: "Characterization of porous silicon by positron lifetime spectroscopy"
R.M. de la Cruz, R.Pareja

G15: "Positron trapping in electron irradiated gallium arsenide"
F.Pierre, C.Corbel, P.Moser, P.Hautojärvi

G16: "Shallow positron traps in gallium arsenide"
S.Dannefaer, P.Mascher, D.Kerr

G17: "Positron annihilation in alloy semiconductors and GaAs"
M.Numata, M.Matsuoka, T.Shimizu, M.Matsui, M.Doyama, T.Hibiya, M.Watanabe

G18: "Shallow positron traps in GaAs"
K.Saarinen, P.Hautojärvi, A.Vehanen, R.Krause, G.Dlubek

Posters: Ionic crystals: . ICPA-8, (19**), Gent.

I20: "Relation between positron lifetimes and resistivity in lightly La-doped BaTiO3"
Tang Chaoqun, Tan Deshang, Zhou Guoliang

I21: "Measurements of positron lifetime and Dopplerbroadening of annihilation gamma line
in ferro- and antiferroelectric crystals at different temperatures"
T.Trosev, Ch.Angelov

I22: "A research of microscopical structure in mullite brick on positron
annihilation technology"
Zou Liu-juan,, Zhang Cai-Guo, Wang Xi-Tang, Li Nan

I23: "A study of defects in metal oxides by positron annihilation"
M.Forster, J.N.Mundy, H.E.Schaefer

I24: "Positron diffusion and annihilation in TiO2 ultrafine powders"
Yuan-jin He, Min Huang, Hui Pan, Hui-jing Chen

I25: "A study of sintering processes in ZnO"
J.del Rio, P.Fernandez, N.de Diego, J.Llopis

I26: "Surface effects on positron annihilation characteristics in CAB-O-SIL (SiO2)"
F.H.Hsu, M.J.Shao, L.O.Hulett, T.M.Rosseel, J.M.Dale

I27: "Evidence for (4:1) defect clustering in COO revealed by 2D-ACAR measurements"
T.Chiba, T.Akahane

I28: "Study of positronium states in KI by using magnetic field"
T.Hyodo, M.Kakimoto, Y.Nagashima, K.Fujiwara

I29: "Positron bound state in the vacancies in alkali halides"
S.B.Nurmagambetov

I30: "Positron annihilation study of irradiation effects in ionic
crystals at the low temperature region"
C.A.Eleftheriades, S.Dedoussis, M.Chardalas, S.Charalambous

I31: "Positron annihilation in ternary graphite intercalation compounds"
H.Murakami, M.Sano, I.Kanesawa, T.Enoki, H.Inokuchi

I40: "Relaxation of the momentum distribution of free positronium atoms
interacting with silica fine particles"
T.Chang, J.Dang, M.Kakimoto, T.Hyodo, T.Akahane, T.Chibe, B.T.A.McKee, A.T.Stewart

I41: "Study of Gd3Ga5O12 crystal doped with Ca2+ by positron annihilation"
Huang Maorong, He Yongshu, Gu Hua, Zhang Lehui, Li Changtian, Liu Hairun

I42: "Study of KCl coloration center crystal by positron annihilation"
Huang Maorong, Gu Hua, Zhou Guangmin, Yang Juhua, Lin Jianmin, Xu Changhuang

I43: "An investigation of the nature of the middle lifetime component of
positron annihilation in teflon"
Wang Shu-Yi, Chang Tianbao